Review | Received 9 June 2026; Revised 18 July 2026; Accepted 5 August 2026; Published 3 September 2026
https://doi.org/10.55092/la20260009

Recent advances in interfacial analysis for biological soft matter using scanning probe microscopy

Rui-Zhi Liu[1,2] and Rui Wen[1,2,*]

[1] Key Laboratory of Molecular Nanostructure and Nanotechnology, Beijing National Laboratory for Molecular Sciences, CAS Research/Education Center for Excellence in Molecular Sciences, Institute of Chemistry, Chinese Academy of Sciences, Beijing, China
[2] University of Chinese Academy of Sciences, Beijing, China

* Correspondence author; E-mail: ruiwen@iccas.ac.cn.

Highlights:

- The application of scanning probe microscopy for biological soft matter interface analysis is reviewed.
- The roles of SPM, mechanical, and bioelectrochemical analysis of soft matter bioanalysis are summarized.
- Hybrid SPM for multidimensional biological interface analysis is discussed.

Abstract: Biological soft matter interfaces govern many biochemical reactions, cellular processes, and disease-related phenotypes, yet their nanoscale mechanical and electrochemical properties remain difficult to measure under native or near-physiological conditions. Conventional ensemble and optical methods provide valuable molecular information, but they often lack the spatial resolution, label-free capability, or non-destructive operation needed to resolve dynamic interfacial processes. Scanning probe microscopy (SPM) addresses this gap by leveraging localized probe-sample interactions to map topography, mechanics, ionic conductance, and electrochemical fluxes at biological soft-matter interfaces. This review summarizes recent progress in atomic force microscopy, scanning electrochemical microscopy, and scanning ion-conductance microscopy for bioanalytical applications. We first outline the operating principles of these representative SPM techniques, then discuss their use in nanoscale mechanical characterization, molecular interaction analysis, single-cell electrochemical imaging, and metabolic monitoring. We further highlight integrated SPM platforms that combine force or ion-current feedback with spectroscopic and fluorescence readouts to link physical structure with chemical function. Together, these developments suggest that SPM-based approaches may provide a versatile route for non-invasive, multidimensional measurements of soft-matter interfaces and offer new opportunities for bioanalysis, disease research, and precision biomedical technologies.

Keywords: scanning probe microscopy; biological soft matter; interface; biomechanics; bioelectrochemistry

1. Introduction

Bioanalytical chemistry provides an experimental foundation for understanding life processes, diagnosing disease, and developing biomedical interventions [1,2]. Contemporary life sciences are increasingly oriented toward connecting molecular information with cellular behavior, tissue function, and pathological progression. Understanding the spatial localization of biochemical events, the regulatory influence of local environments, and the evolution of these processes within living or biomimetic systems is important [3]. Crucially, biological soft matter interfaces are the primary platform for addressing this analytical challenge, providing the hydrated, deformable, and chemically heterogeneous environments required for complex biological regulation. These interfacial regions, which encompass cell membranes, extracellular matrices, and hydrogels, are not passive boundaries but dynamic scaffolds where physical processes, such as mass transport and charge transfer, are integrated with biochemical functions, including signaling, receptor activation, and molecular recognition [4]. Elucidating these interfacial interactions may provide useful insights for refining disease diagnostics and accelerating the development of targeted therapeutic interventions.

Current research in soft matter bioanalysis centers on two core scientific problems. First, the mechanism of microscopic charge transfer and conduction within biological systems requires further elucidation, as it underpins essential cellular activities. Second, the correlation between local mechanical properties and complex pathological symptoms requires investigation, given that mechanical microenvironments drive disease progression. Investigating these fundamental issues can help reveal mechanisms such as gene transcription, protein folding, and drug-target interactions. Consequently, addressing these problems may provide an experimental basis for optimizing targeted therapies and achieving early precision diagnosis.

Decoding these complexities requires non-invasive, multimodal measurement techniques operating under near-physiological conditions [5,6]. Liquid chromatography-mass spectrometry enables sensitive molecular identification and quantitative profiling, while fluorescence microscopy provides molecular specificity and dynamic visualization in cells and tissues [7]. Spectroscopy, bulk electrochemistry, electron microscopy, and optical imaging also provide valuable insights into composition, kinetics, ultrastructure, and physiological responses. These methods form the current backbone of bioanalytical research. At the same time, their greatest advantages usually lie in chemical coverage, molecular selectivity, throughput, field of view, or structural visualization, rather than in simultaneous local measurement of soft interfacial topography, mechanics, ion conductance, and electrochemical flux [8]. Scanning probe microscopy (SPM) has emerged to address these needs by leveraging probe-sample interactions to characterize mechanical and electrical parameters with high precision [9]. By enabling the simultaneous detection of topography, mechanics, and electronics, SPM has become a valuable tool for multi-parameter biological measurement, as shown in Figure 1. Among the diverse family of SPM techniques, Atomic Force Microscopy (AFM), Scanning Electrochemical Microscopy (SECM), and Scanning Ion-Conductance Microscopy (SICM) are selected here as the most representative and complementary triad for soft matter analysis. This selection is driven by a clear rationale: biological soft matter, a complex interplay of mechanical properties and electrochemical processes, inherently governs interfaces. AFM quantifies nanomechanical attributes (such as viscoelasticity and molecular binding forces); SECM excels at tracking localized chemical activity and metabolic redox fluxes; and SICM provides unparalleled,

non-contact topographic mapping and ionic conductance measurements in native liquid environments without introducing mechanical perturbation. Together, they form a comprehensive framework capable of capturing the full physical-chemical landscape of delicate biological specimens.

Here, this review focuses on AFM, SECM, and SICM as representative SPM techniques, as they provide a complementary set of readouts for biological soft-matter interfaces. AFM directly probes nanoscale topography, mechanics, and molecular interaction forces in hydrated soft systems; SECM maps local electrochemical activity and metabolic flux through current responses at ultramicroelectrodes; and SICM uses ion-current feedback for non-contact imaging of fragile living interfaces and ion-transport behavior. These techniques were selected to address the principal interfacial variables governing biological soft matter: morphology, mechanics, charge/ion transport, and chemical reactivity. The main contribution of this review is therefore to integrate the SPM into a unified framework for the analysis of biological soft-matter interfaces. Rather than treating each technique as an isolated instrumentation topic, we organize recent advances around biological questions, including nanoscale mechanical and bioelectrochemical reactions, cellular metabolism, and hybrid physicochemical imaging. This perspective clarifies how SPM can be combined to connect local interfacial properties with biological function, disease phenotypes, and biomedical applications.

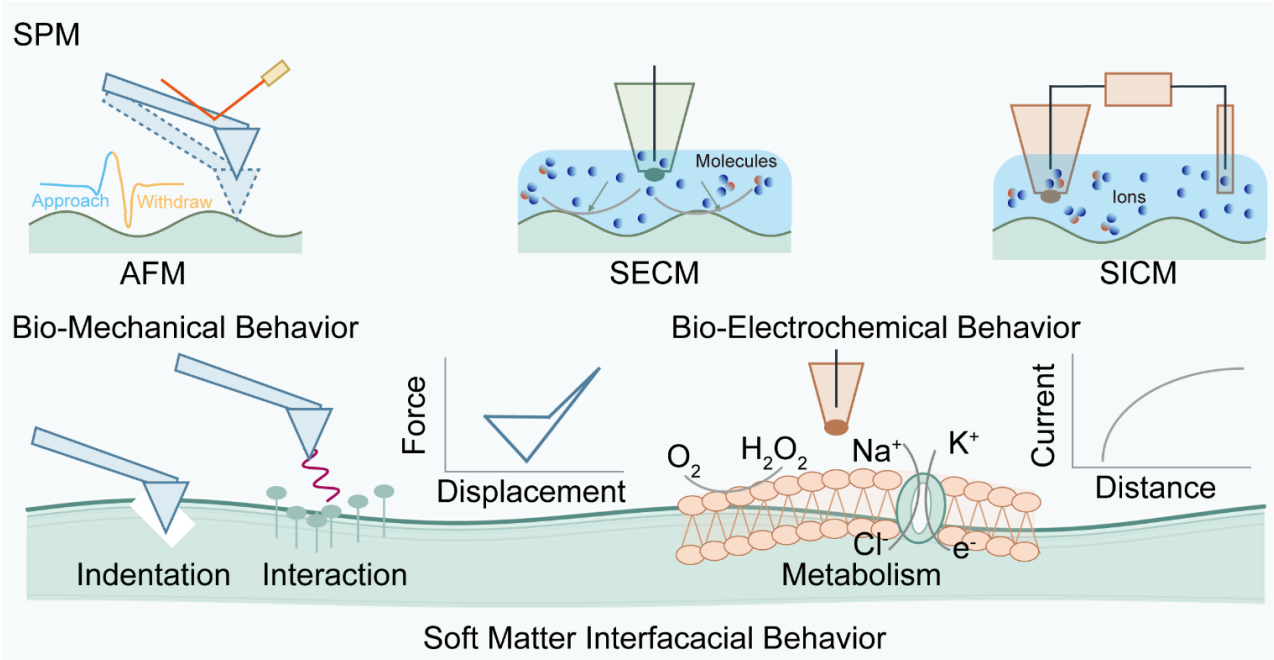

Figure 1. SPM is used to probe the interfacial behavior of biological soft matter.

2. The fundamental principles of SPM techniques

Measuring soft-matter interfaces in biological systems requires techniques that provide high spatial resolution without disrupting native structure. SPM meets this need by monitoring local interactions between a sharp probe and the sample surface, allowing nanoscale imaging in air or liquid environments [10]. Consequently, SPM has been extensively used to characterize biological soft-matter interfaces [11,12]. Within this field, AFM, SECM, and SICM have garnered significant research interest due to their high sensitivity to mechanical and electrochemical signals, respectively. The following section will detail the fundamental principles governing these three representative SPM techniques.

2.1. AFM

AFM has established itself as a cornerstone for nanoscale characterization, particularly for biological soft interfaces in surface science, materials science, and biomedicine [13,14]. At its core, AFM utilizes a nanoscale tip attached to a cantilever. Its movement is monitored by a laser deflection system that reflects a beam from the cantilever's backside onto a photodiode, a configuration that enables the acquisition of both topographic data and mechanical properties [15,16]. Among mechanical properties, the elastic modulus is the most prevalent physical quantity for describing soft interfaces at the nanoscale, representing the material's resistance to deformation. In the context of cancer diagnosis, the modulus can serve as an informative mechanical biomarker [17]. Specifically, by performing nanoindentation experiments across selected regions, researchers can map modulus distributions to distinguish malignant cells from their healthy counterparts based on their distinct mechanical signatures [18]. To quantify these data, the Hertzian mechanics model is widely applied. This model relates force and indentation through the following equation: $F = ch^m$, where F represents the interaction force between the probe and the sample, h denotes the indentation depth, c is a parameter determined by the material's mechanical properties (such as Young's modulus and Poisson's ratio) and the probe geometry, and m is a constant dictated solely by the probe's shape [19,20]. Through statistical fitting, multiple mechanical parameters of the sample can be estimated.

Beyond conventional AFM applications, high-speed AFM (HS-AFM) has become a useful tool for biologists, offering sub-second temporal resolution and high spatial resolution to observe the real-time structural dynamics of biomolecules. As shown in Figure 2a, the scanning speed of traditional AFM is primarily restricted by the mechanical bandwidth and response delays of its core components, such as the cantilever and piezoelectric scanner [21]. To overcome these physical limitations, HS-AFM employs system-level design optimizations to minimize signal processing latency [22]. At the probe level, HS-AFM employs miniaturized, high-frequency cantilevers that achieve megahertz resonance frequencies while maintaining low spring constants to prevent sample damage [23]. In terms of hardware, traditional mechanical structures are replaced by high-frequency scanners based on flexure hinges or tripod designs, supported by wide-bandwidth power amplifiers. To further accelerate feedback, HS-AFM incorporates peak-hold circuits or wide-bandwidth lock-in amplifiers for rapid amplitude and frequency estimation [24].

Additionally, the use of spiral or cycloid scanning trajectories, rather than traditional triangular raster patterns, suppresses mechanical resonance errors [25]. Due to these advancements, HS-AFM can efficiently assess the structural and dynamic features of single, label-free protein molecules in action with high spatiotemporal resolution. This approach bypasses the static ensemble averaging of traditional structural biology and the optical labeling requirements of single-molecule biophysics. The technology has been successfully applied to various protein systems, achieving *in situ* structural imaging of relatively rigid higher-order structures, such as the dense diffusion of bacterial outer membrane porin trimers, aquaporin arrays in lens cell membranes, and protein fluctuations within nuclear pore complex channels.

2.2. SECM

SECM employs an ultramicroelectrode (UME) as a probe to detect electrochemical reaction currents between the sample and the probe, thereby characterizing the chemical activity of the material surface [16].

A distinctive feature of the UME is its ability to reach an electrochemical steady state rapidly. The steady-state current equation quantifies this:

$$i = 4nFr_0Dc \quad (1)$$

where n is the number of electrons transferred, F is the Faraday constant, r_0 is the radius of the disk UME, D is the diffusion coefficient, and c is the concentration; this differs from the time-dependent current at macro-electrodes, $i = nAFc(D/\pi t)^{0.5}$, which depends on the electrode area A and time t [26]. This rapid attainment of a steady state makes the UME a useful tool for analyzing chemical reaction kinetics. Due to its exceptional sensitivity to chemical processes, SECM has been extensively used to monitor ion transfer at the liquid-liquid interface, visualize local catalytic activity, and perform bioelectrochemical measurements at soft-matter interfaces [27].

Typically, SECM characterizes substrate chemical activity using current-feedback and GC modes, as shown in Figure 2b,c [28]. In the current feedback mode, when the probe is far from the substrate, the diffusion profile is hemispherical. When the probe approaches a conductive substrate, the current is enhanced by redox cycling between the probe and the substrate, resulting in positive feedback. Conversely, as the probe approaches an insulating substrate, the current decreases because the substrate's presence impedes the diffusion of reactants from the bulk solution to the electrode surface, leading to negative feedback. In the generation-collection mode, the reciprocal generation and consumption of active species between the probe and the substrate enable effective detection of surface active sites [29].

2.3. SICM

A typical SICM system comprises a nanopipette serving as the scanning probe, a piezoelectric actuator, a current amplifier for recording ion currents, and auxiliary electronics including a data acquisition system and a scanning controller, as shown in Figure 2d [30]. The fundamental operation of the SICM relies on using a nanopipette to sense the topography and properties of the sample surface by monitoring ion current flow, thereby enabling non-contact imaging at the nanometer scale. An ion current (I) is generated by applying a bias voltage (U) between an electrode inside the nanopipette and a reference electrode (RE) situated in the surrounding electrolyte. When the nanopipette approaches the sample, the substrate's physical presence restricts ion flux, making the current highly sensitive to the probe-to-sample separation. This sensitivity enables the current to serve as a precise feedback signal to control the distance between the tip and the sample, facilitating measurements at soft-matter interfaces. When the nanopipette is positioned far from the substrate, a steady-state ion current (I_∞) is recorded. The relationship between the ion current and the separation distance can be characterized by the following equation, as shown in Figure 2e:

$$I = \frac{U}{R_p + R_z} \approx I_\infty \left(1 + \frac{1.5 \ln\left(\frac{r_0}{r_i}\right) r_i r_e}{hd}\right)^{-1} ; \; I_\infty = \frac{U}{R_p} \quad (2)$$

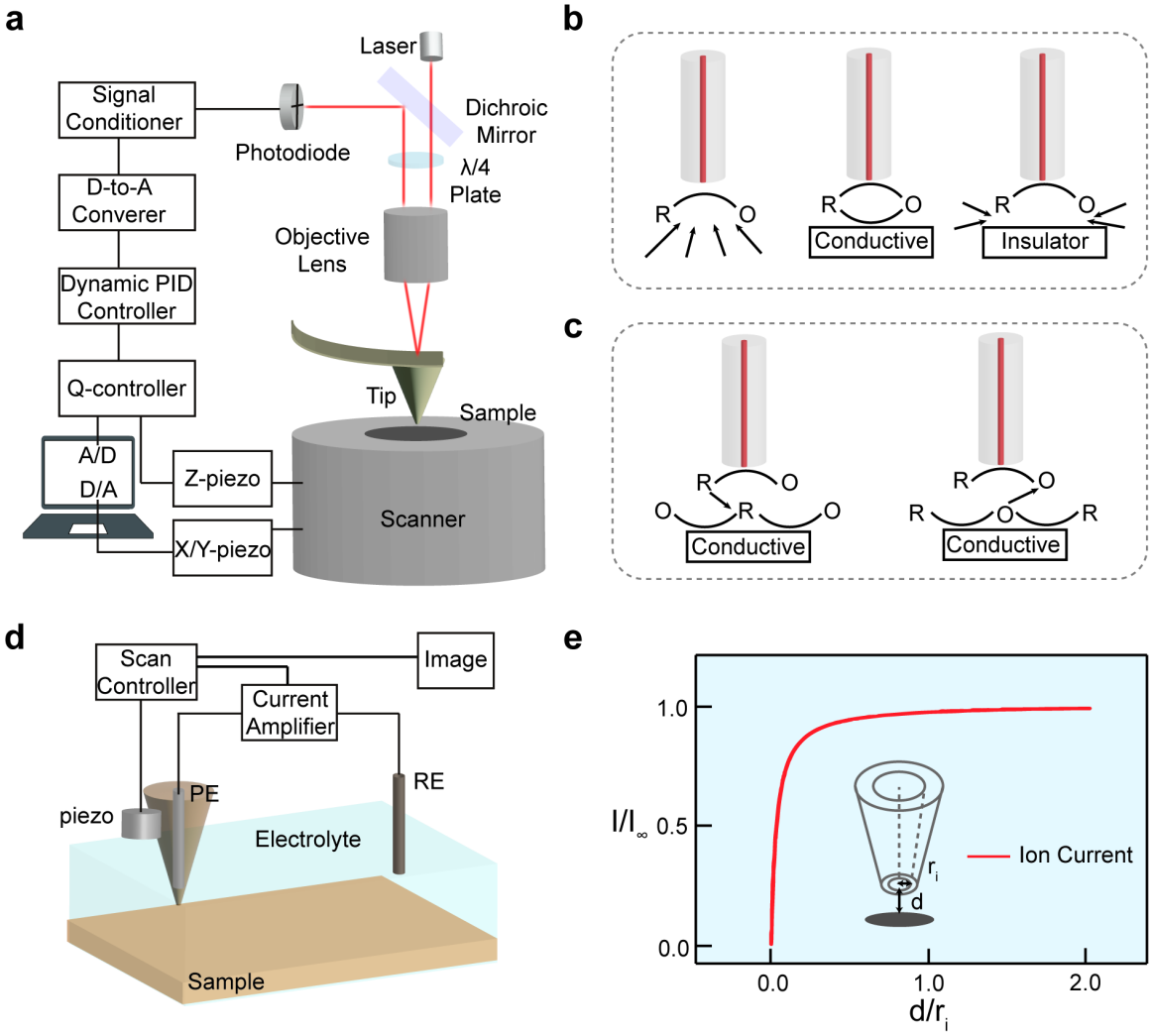

Figure 2. Working principles of representative SPM techniques. **(a)** Scheme of HS-AFM; **(b, c)** Current-feedback and generation-collection modes in SECM; **(d)** Scheme of SICM; **(e)** Relationship between ion current and tip-sample distance.

To acquire a topographical map of the sample surface, the system typically employs a constant-current feedback mode. Specifically, the scanning controller utilizes a feedback algorithm to maintain a pre-defined constant percentage decrease in the ion current relative to I_{∞}. The piezoelectric actuator adjusts the probe's vertical position to keep the current setpoint constant while scanning laterally, and the resulting vertical displacements are recorded to reconstruct the surface morphology [30]. In signal collection, the selection of electrodes and electrolytes is important for maintaining signal stability. For RE, Ag/AgCl electrodes are the standard choice due to their ability to maintain a stable reference potential over long experimental durations. Pt or Pd electrodes are used in specific systems where Ag/AgCl might cause ionic contamination [31]. Among electrolytes, KCl is preferred because K^+ and Cl^- have nearly equal transference numbers. This leads to balanced ion flux and minimizes liquid junction potentials. What's more, physiological buffers and culture media, such as Phosphate-Buffered Saline (PBS), are widely used in SICM studies of biological specimens to ensure biocompatibility [32]. While AFM, SECM, and SICM offer distinct advantages for nanoscale characterization, each technique is subject to critical, probe-related limitations that can compromise data integrity, as shown in Table 1.

Table 1. Evaluation of performance metrics of AFM, SECM, and SICM techniques in biosystems.

	AFM	SECM	SICM
Measurable Signal	Tip-sample mechanical forces	Ultramicroelectrode Faradaic current	Nanopipette orifice ion current
Spatial Resolution	Vertical: ≤ 0.1–1 nm Horizontal: ≤ 1–10 nm	Vertical: ≤ 10 nm Horizontal: ≤ 10–100 nm	Vertical: ≤ 1 nm Horizontal: ≤ 10–50 nm
Temporal Resolution	AFM: minutes/frame HS-AFM: several frames/second	minutes/frame	minutes/frame
Operation Environment	Air, liquids, ultra-high vacuum	Electrolyte/redox mediator liquids	Ionically conductive liquids
Detection Sensitivity	pN-level forces	pA-level molecular fluxes	pA-level ion current shifts
Live-Cell Compatibility	Low to moderate (Tip damage)	Moderate (Chemical cytotoxicity)	High (non-contact, mediators' cytotoxicity)
Advantages	• Nanometer topography • Simultaneous mechanical mapping	• High chemical specificity • Quantitative redox kinetics	• Non-contact topography preservation • Local ion concentration mapping
Limitations	• Tip-induced specimen damage	• Complex electrode fabrication & functionalization	• Nanopipette clogging in complex bio-systems

In AFM, the primary artifact arises from the physical tip-sample contact force, which inevitably deforms ultra-soft living specimens, leading to significant topography distortion and underestimation of cell height. Furthermore, high-resolution imaging often accelerates tip wear or results in biomolecular fouling, which blurs the recorded morphology. For SECM, a major limitation lies in the convolution of topographical and electrochemical signals; because the Faradaic current depends heavily on both the local chemical flux and the absolute tip-to-sample distance, structural variations can be misinterpreted as chemical activity unless complex decoupling modulation is applied. Additionally, fabricating reproducible nanoscale ultramicroelectrodes remains highly challenging. In the case of SICM, although it is a non-contact method, it is highly prone to probe-related artifacts, such as nanopipette clogging, which frequently occurs when scanning complex, high-salt, or mucilage-heavy biological systems. This clogging disrupts the steady-state ion-current feedback, causing spurious topographical spikes or complete system crashes. Moreover, SICM remains inherently incapable of directly mapping mechanical parameters such as stiffness or surface adhesion, thereby restricting its utility strictly to morphological and ion-flux tracking. These distinct artifacts and operational boundaries must be carefully accounted for in the analysis of any biological or chemical imaging data.

3. Nanoscale mechanical characterization at biological soft matter interfaces

Mechanical behavior at soft-matter interfaces is central to materials science, biomedical engineering, and mechanobiology. Soft systems, including hydrogels, living cells, and biomacromolecule assemblies, are dynamic, heterogeneous, and sensitive to environmental factors such as temperature, pH, and ionic strength [33,34]. Accurately characterizing their micro- and nanoscale mechanical properties, such as Young's modulus, viscoelasticity, interfacial adhesion, and receptor-ligand binding forces, is important for developing targeted drug delivery systems, designing biomimetic scaffolds, and elucidating the mechanisms underlying diseases such as cancer. While traditional macroscopic methods, such as uniaxial compression or rheometers, provide bulk mechanical data, they lack the spatial resolution needed to capture the local mechanical gradients and heterogeneities inherent in soft interfaces. To

overcome these limitations, AFM has emerged as a cornerstone technology. Its ability to operate nearly non-destructively in physiological fluids, combined with nanometer-scale spatial resolution and piconewton-level force sensitivity, has made AFM particularly useful in biological soft matter research.

3.1. Nanomechanical behavior and evolution of biological soft matter interfaces

AFM nanomechanical measurements primarily rely on the acquisition and analysis of force-distance curves. Mechanical analysis in AFM has utilized established contact mechanics models to interpret these curves, with the Hertz model being the most widely applied due to its simplicity. However, most soft materials, such as hydrogels and tissues, are complex viscoelastic systems that exhibit stress relaxation and creep under varying indentation rates. This viscoelastic nature means that applying purely elastic assumptions often leads to significant non-linear offsets in calculated moduli, thereby compromising the objective assessment of intrinsic mechanical properties. To address this, Antonio Minopoli *et al.* [17] developed a framework based on Standard Linear Solid (SLS) and Kelvin-Voigt models to isolate elastic and viscous contributions, as shown in Figure 3a. They conducted comprehensive AFM tests on four hydrogels (Alginate, Cellink-RGD (alginate covalently conjugated with RGD, the cell-attachment peptide sequence, and nanofibrillated cellulose), GelMA (gelatin methacrylated), and GelMA A (a blend of GelMA and alginate)) using conical silicon probes at gradient indentation rates from 0.5 to 15 μm/s. The results showed that the apparent Young's modulus for all samples increased nonlinearly with the indentation rate before reaching an elastic asymptote. Pure Alginate and GelMA exhibited lower effective viscosities and softer characteristics (~5.7 kPa and ~18.2 kPa, respectively), reflecting loose polymer chains that are capable of rapid spatial rearrangement.

In contrast, Cellink-RGD and GelMA A showed stiffness increases of several orders of magnitude (350–400 kPa) and high effective viscosity. This suggests that their densely interpenetrating and cross-linked networks generate strong synergistic reinforcement; these structures create significant internal friction under rapid loading, effectively "freezing" the microstructure and dissipating energy through viscous drag rather than elastic storage. These quantitative laws may provide useful guidance for 3D bioprinting inks designed to mimic tissues ranging from soft brain matter to stiff cartilage.

Polymer brushes consist of macromolecular chains densely grafted to a substrate, where steric hindrance forces the chains to extend outward [35]. These interfaces can reversibly swell or collapse in response to external stimuli, modulating adhesion, friction, and antifouling performance. Characterizing these nanometer-thick, ultra-soft layers requires care, as sharp probes can easily penetrate the brush and encounter the stiff underlying substrate. Asya Eroğlu *et al.* [36] demonstrated this by using surface-initiated photoinduced electron transfer-reversible addition-fragmentation chain transfer (PET-RAFT) polymerization to synthesize dual-responsive poly(acrylic acid)-co-poly(N-isopropylacrylamide) (PAA-co-PNIPAm) brushes. AFM experiments confirmed the independent responsive nature of the blocks: PAA chains extended at higher pH due to electrostatic repulsion, while PNIPAm chains collapsed above 30 °C due to increased hydrophobicity. These observations provide useful evidence for the design of smart cell culture substrates and functional films with controllable molecular-capture capabilities.

Furthermore, Maxim E. Dokukin *et al.* [37] proposed a decoupling model to simultaneously quantify brush molecular parameters and substrate mechanics by partitioning the indentation process into steric repulsion and elastic substrate zones, as shown in Figure 3b–d. Using the poly(ethylene oxide) (PEO) and cross-linked poly(2-vinylpyridine) (P2VPxl) system, they obtained estimates of substrate moduli

(~20–50 MPa) and brush thickness (~16–19 nm) across different pH values. Despite a 50% deviation in absolute grafting density due to chain interpenetration and solvent effects, this model offers a rigorous framework for studying pericellular brushes and responsive soft interfaces.

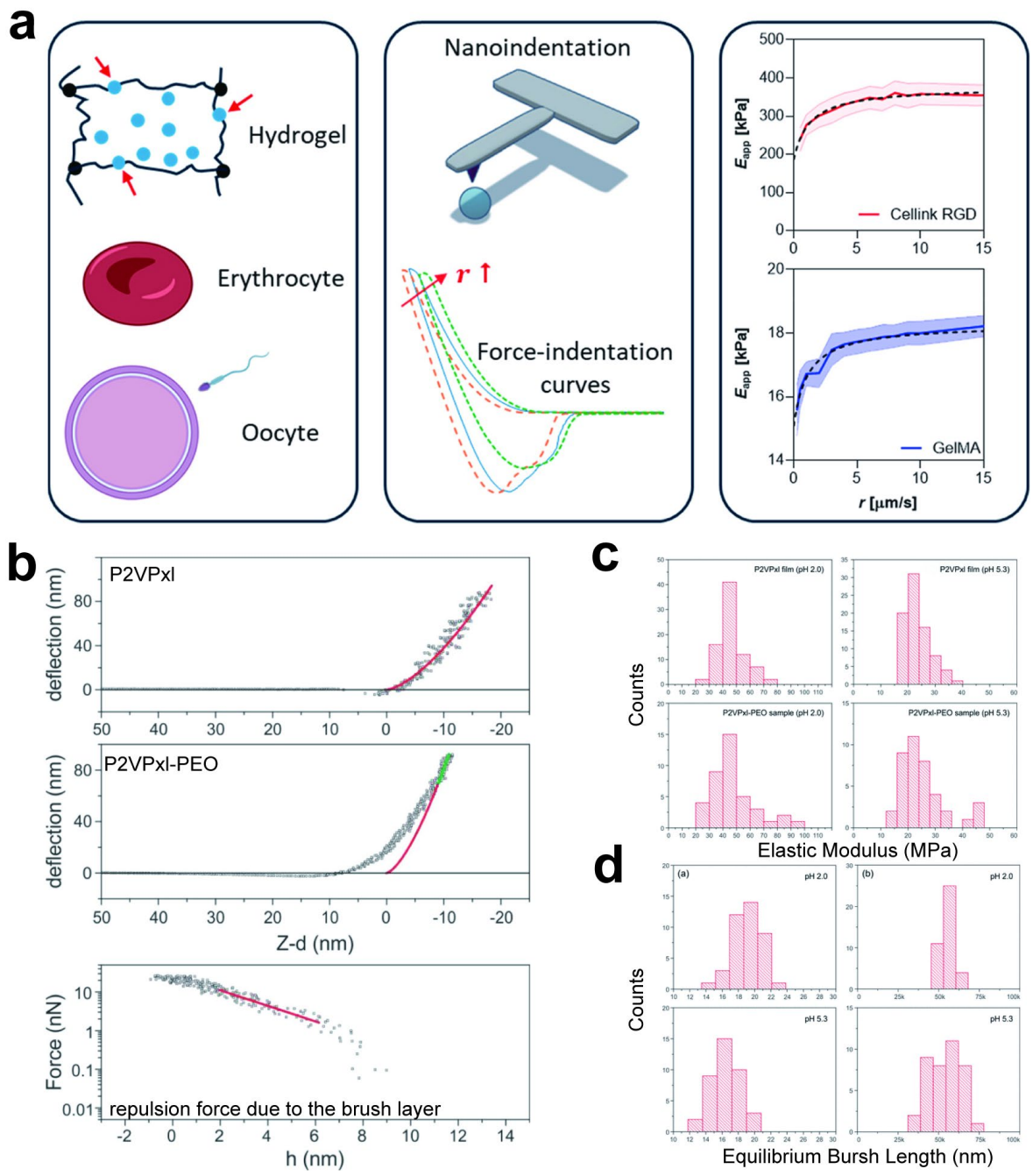

Figure 3. AFM nanomechanical analysis of hydrogels and polymer brushes. **(a)** AFM cantilever with a conical tip probing a hydrogel and apparent Young's modulus of Cellink-RGD and GelMA A as a function of indentation rate. Solid lines show estimated apparent Young's modulus over 64 measurements, and shaded areas show standard deviations. Reprinted with permission [17]. Copyright 2025 The Authors; **(b)** Fitting of bare P2VPxl and P2VPxl-PEO samples, with the lower panel showing repulsive force from the PEO brush; **(c)** Elastic modulus histograms for P2VPxl and P2VPxl-PEO at two pH values; **(d)** Distributions of PEO brush length and grafting density derived for P2VPxl-PEO at two pH values. Reprinted with permission [37]. Copyright 2017 American Chemical Society.

3.2. Detection of molecular interactions at biological soft matter interfaces

The versatility of AFM extends to the study of living cells, where it serves as a high-precision tool for mapping the global mechanical state and specific molecular interactions that underpin immune functions. Cell mechanics and surface receptor distributions reflect physiological health and govern environmental sensing, migration, and proliferation. Xiaohong Fang's team has been conducting continuous research on molecular interactions for many years. They investigated the dissociation kinetics and multivalent energy landscapes of the specific interaction between a bivalent aptamer (Bi-8S) and thrombin, as shown in Figure 4a [38]. This bivalent aptamer comprises 15 apt and 27 apt, which bind to exosite I and exosite II of thrombin, respectively, and are linked by eight spacer phosphoramidites. The researchers covalently modified the AFM tips with thrombin and immobilized the aptamers onto silicon substrates for single-molecule force spectroscopy (SMFS) characterization. SMFS combined with specific blocking experiments indicated that the force-driven unbinding of this bivalently bound system follows a sequential dissociation mechanism. Dynamic force spectroscopy (DFS) data further revealed that within Bi-8S, the presence of the eight spacers leaves the binding characteristics of 27 apt to thrombin exosite II virtually unaffected; however, the spacer significantly stabilizes the binding of 15apt to exosite I, reducing its unstressed dissociation rate (k_0) by up to two orders of magnitude, thereby substantially prolonging the lifetime of the complex. This finding supports the possibility that flexible linkage structures can optimize multivalent binding efficiency by modulating molecular conformational states, providing critical micromechanical and kinetic parameters for the rational design of high-affinity nucleic acid therapeutics. Similarly, to develop novel pathogen-targeting probes capable of replacing high-cost and low-stability antibodies, they demonstrated that the endolysin cell wall binding domain, PlyV12C, possesses ultra-high recognition affinity and mechanical stability comparable to conventional antibodies: SMFS measured the dissociation force of PlyV12C at 45.3 ± 1.4 pN *in vitro* (on purified peptidoglycan) and 52.3 ± 2.0 pN (on the envelope of *S. aureus*), which is highly close to the binding force of a monoclonal antibody (56.7 ± 0.9 pN). Furthermore, DFS revealed dual linear regimes for both systems, suggesting that their unbinding pathways may involve two sequential transition-state energy barriers, as shown in Figure 4b,c [39]. This supports the potential use of PlyV12C as an alternative to conventional antibodies as high-affinity probes for rapid clinical biosensing and detection of drug-resistant strains.

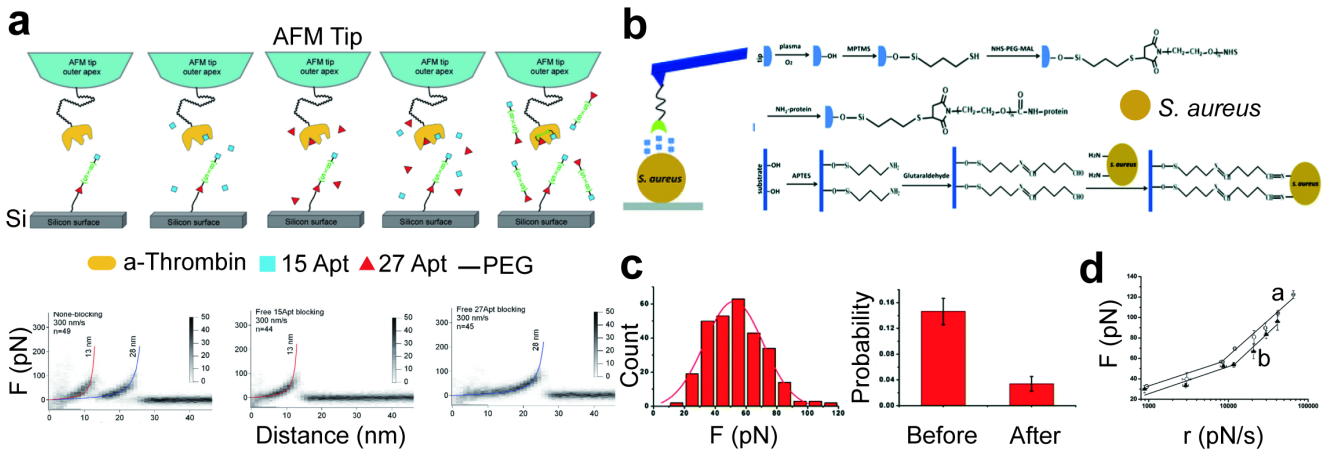

Figure 4. AFM force spectroscopy for probing specific molecular interactions at soft-matter biointerfaces. **(a)** Schemes for the mechanical unbinding of thrombin/aptamer complexes. Superimposition of force-distance curves recorded at a pulling speed of 300 nm/s in buffer solution without blocking aptamer, with free 15 aptamer blocking, with free 27 aptamer blocking, with both free 15 and 27 aptamer blocking, and with free Bi-8S aptamer blocking. The buffer solution used was 140 mM NaCl, 5 mM KCl, 1 mM $CaCl_2$, 1 mM $MgCl_2$, and 20 mM Tris-HCl at pH 7.4. The concentration of free aptamer for blocking is 1.0×10^{-7} M in buffer. Reprinted with permission [38]. Copyright 2011 American Chemical Society; **(b)** Functionalization of the AFM tip with PlyV12C/antibody and immobilization of *S. aureus* on the silicon substrate; **(c)** Interaction forces between PlyV12C and peptidoglycan on *S. aureus* cells probed by AFM-SMFS; **(d)** Comparison of dynamic force spectra of antibody-*S. aureus* and PlyV12C-*S. aureus*. Reprinted with permission [39]. Copyright 2015 Royal Society of Chemistry.

In cellular immunology, AFM-based Single Virus Force Spectroscopy (SVFS) allows researchers to probe interactions between viruses and host receptors at the piconewton level. For instance, Koehler *et al.* [40] used AFM to resolve the entry cascade of Reovirus, finding that initial binding to cell-surface sialic acid triggers a conformational change in the virus attachment protein, as shown in Figure 5a,b. This transition enhances binding to the core receptor junctional adhesion molecule A (JAM-A), forming multiple parallel specific bonds. Fitting these interactions with the Bell-Evans model revealed a dissociation rate of approximately 0.09 ± 0.04 s^{-1}, suggesting that multivalent anchoring slows viral diffusion to facilitate endocytosis. Similarly, Formosa Dague *et al.* [41] used Single-Cell Force Spectroscopy (SCFS) to quantify adhesion between *Staphylococcus aureus* and human corneocytes. Comparisons between wild-type and mutant strains showed that the absence of cell wall-anchored (CWA) proteins led to a total loss of adhesion, while single-cell binding forces averaged 500 pN due to multiple specific adhesin-ligand interactions, as shown in Figure 5c. Knoops *et al.* [42] confirmed that extracellular Peroxiredoxin-5 (PRDX5) acts as a damage-associated molecular pattern (DAMP) by binding specifically to Toll-like receptor 4 (TLR4) receptors, as shown in Figure 5d. AFM measured single-pair rupture forces between 30 and 60 pN; notably, receptor activation caused THP-1 or Chinese hamster ovary (CHO) cells to stiffen significantly within 15–30 minutes. This mechanical shift, driven by cytoskeletal reorganization downstream of receptor signaling, reveals a potential micromechanical trigger for the tissue stiffening observed in inflammatory diseases such as atherosclerosis.

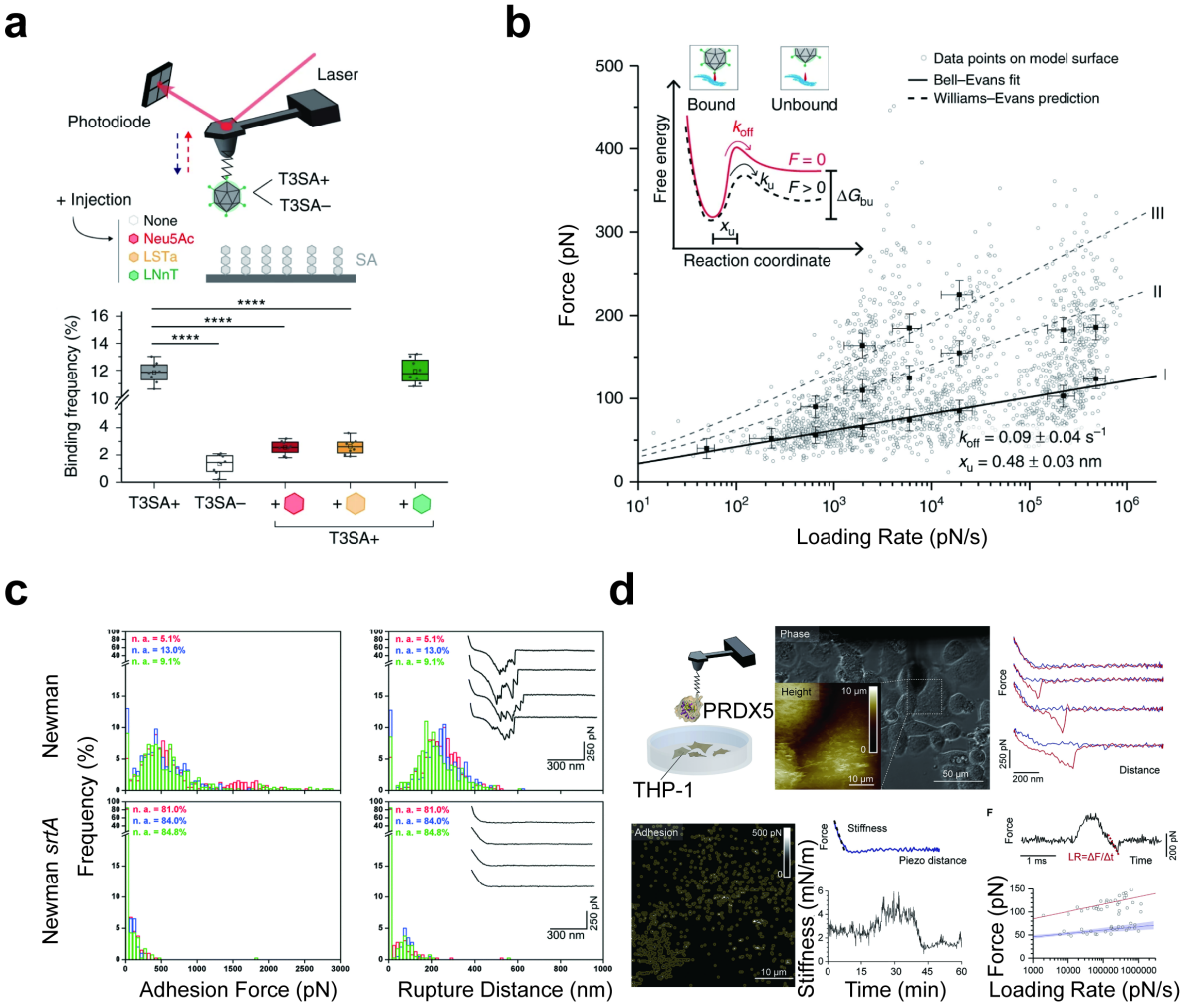

Figure 5. AFM-based force spectroscopy for analyzing pathogen-host and immune receptor interactions. **(a)** Binding of single virions is probed on an SA-coated surface in the presence or absence of α-SA glycan derivatives, and the box plot of specific binding frequencies measured by AFM between virions and α-SA before and after injection of 1 mM glycans; **(b)** DFS plot showing the distribution of rupture forces measured between $T3SA^+$ and the SA-coated surface (gray dots) with average rupture forces determined for eight distinct loading rate (LR) ranges. Reprinted with permission [40]. Copyright 2019 The authors; **(c)** Adhesion force and rupture distance histograms with representative force profiles obtained in PBS between *S. aureus* Newman bacteria and corneocytes. Adhesion force and rupture distance histograms with representative force profiles obtained between *S. aureus* Newman srtA and corneocytes. Reprinted with permission [41]. Copyright 2016 Royal Society of Chemistry; **(d)** Mapping PRDX5 Binding to Macrophage-Differentiated THP-1 Cells Using Correlative Wide-Field Microscopy and FD-Based AFM. Reprinted with permission [42]. Copyright 2018 Elsevier Ltd.

4. Nanoscale bioelectrochemical analysis at soft matter interfaces

In the life sciences, basic medicine, and pharmacology, investigating electrochemical reaction mechanisms at biological soft-matter interfaces is important for understanding life processes and addressing diseases [43]. Traditional ensemble methods are often limited by their destructive nature, which requires cell lysis and fails to capture the authentic state of biomolecules or resolve fine

topological structures at the nanoscale. Given that cellular metabolism and signaling occur across complex, multi-phase interfaces, non-invasive bioelectrochemical analysis with high spatiotemporal resolution is imperative [44,45]. SPM and its derivatives, such as SECM, SICM, and Scanning Electrochemical Cell Microscopy (SECCM), may provide a useful platform to meet these needs. By exploiting near-field interactions between the probe and the biological surface, such as Faraday currents and ionic conductance, SPM enables the simultaneous quantitative detection of topography, mechanics, and electrochemical fluxes. This bridges the gap between macroscopic measurements and microscopic dynamics, providing experimental information relevant to precision medicine and targeted drug delivery. To demonstrate the development of SPM in modern bioelectrochemistry, this section reviews recent advances in electrochemical detection at biological soft-matter interfaces.

4.1. Microstructural and electrochemical imaging of targeted proteins on single cells

At the single-cell level, SPM enables label-free electrochemical imaging and precise localization of membrane morphology, local charges, and specific transmembrane proteins. This nanoscale *in situ* observation provides a useful perspective for analyzing receptor functions and secretion dynamics. Dechen Jiang *et al.* [46] used SECCM with a solid-polymer-electrolyte nanopipette probe to investigate the spatial distribution of specific proteins in fixed cell membranes, as shown in Figure 6a. They discovered that carcinoembryonic antigen (CEA) is distributed heterogeneously on the membranes of breast cancer cells (MCF-7). By labeling CEA antibodies with ruthenium complexes and utilizing the high affinity between streptavidin and biotin, the researchers recorded CV within the contact area of a 130 nm nanopipette. Based on potential-resolved peak currents, the method achieved a spatial resolution of 160 nm, overcoming the resolution degradation caused by product diffusion in traditional SECM. The resulting maps showed denser CEA expression at cell edges than at the center.

In summary, this study offers a strategy for super-resolution protein visualization by confining electrochemical reactions within a nanoprobe to eliminate diffusion interference. Yuji Nashimoto *et al.* [47] focused on tracking dynamic processes in living cells without exogenous labels, as shown in Figure 6c,d. They investigated the dynamic exocytosis of unlabeled von Willebrand factor (vWF) in living human umbilical vein endothelial cells (HUVECs). Using SICM, they identified the fine fibrous network of vWF and the transient opening and closing dynamics of secretory pores. vWF exocytosis was induced by stimulating calcium influx with phorbol myristate acetate (PMA). By applying a 200 mV bias to generate an ion current feedback, SICM resolved vWF protein fibers as thin as 60 nm and captured pore movements approximately 500 nm in diameter without artifacts. These findings suggest that non-invasive SICM can effectively visualize microscopic topological changes during live-cell secretion, which may complement optical imaging.

Beyond protein secretion, the evolution of membrane morphology and local electrostatic charge is important in aging. Yao Song *et al.* [48] explored these changes in aging cells by improving SICM mapping methods, as shown in Figure 6b. They found that as human dental pulp stem cells (hDPSCs) age, their surface charge becomes significantly more negative and the cytoskeleton becomes highly disordered. The researchers utilized the electrostatic interaction within the electrical double layer between a charged glass nanopipette and the cell surface to resolve charge density. After validating the mechanism via finite element simulation (FEM), they performed *in situ* scans of hydrogen peroxide-induced senescent hDPSCs. The results showed that while young cells maintain uniform charge and cytoskeleton distribution,

aging cells exhibit altered microvilli and a profound negative shift in membrane electrical properties. This innovative method provides useful evidence for identifying specific stages of cellular senescence using label-free physical parameters.

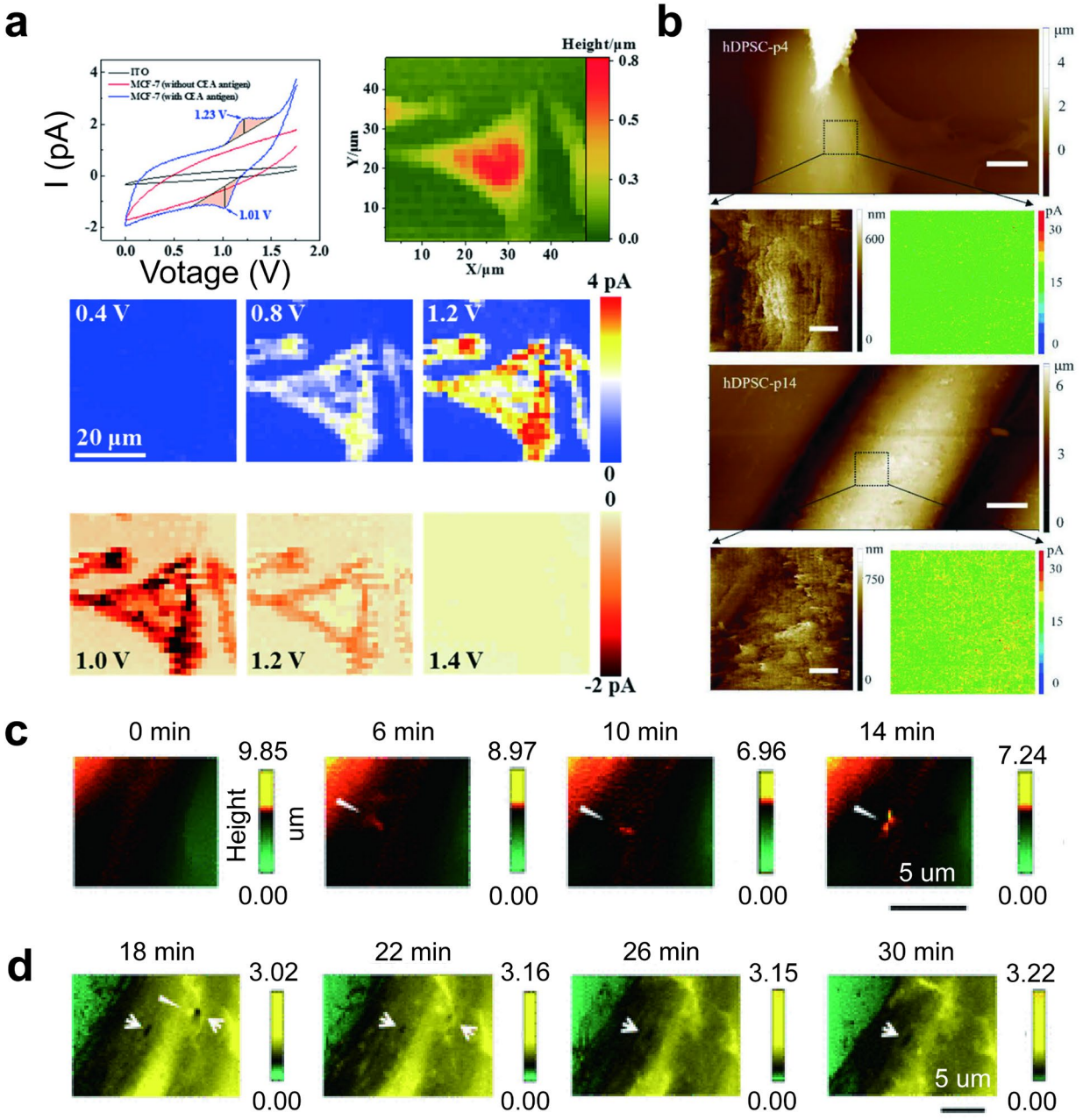

Figure 6. SPM-based nanoscale imaging of membrane proteins, secretion dynamics, and cellular surface charge. **(a)** CV curves from the MCF cells modified with the Ru-tagged antibody, unmodified MCF cells, and the ITO surface. SECCM topographic image of MCF cells. SECCM current image of MCF cells. SECCM current image of MCF cells. Reprinted with permission [46]. Copyright 2023 American Chemical Society; **(b)** Representative images of topography and surface charge (ΔI) of hDPSCs-4 and -p14 (scale bar: 5 μm and 1 μm). Reprinted with permission [48]. Copyright 2023 Wiley-VCH GmbH; **(c)** Imaging of the vWF in living cells. Sequential images of living HUVECs after PMA stimulation. The arrowhead indicated the protrusion; **(d)** The extension of the protrusion. Reprinted with permission [47]. Copyright 2015 American Chemical Society.

4.2. Electrochemical monitoring of the metabolic dynamics of the cell

Electrochemical monitoring of the metabolic state of living cells under environmental stress can provide useful insights into cellular physiology. SECM, characterized by its high sensitivity to redox species, is widely used to detect dynamic flux changes in living cells under various metabolic processes or environmental challenges. Single-cell analysis focuses on achieving high-precision measurements of basal metabolic rates to establish accurate physiological benchmarks. Kelsey Cremin *et al.* [49] measured single-cell respiration rates using SECM. Through pulse-measurement protocols and finite-element simulation analysis, the researchers discovered that the actual oxygen consumption flux of a single cell is significantly lower than the overestimations previously reported in some SECM literature, as shown in Figure 7a.

Furthermore, they noted that the measurement process is highly susceptible to interference from electrode biofouling and probe-induced deprivation effects. Since cellular respiration is a core indicator of energy metabolism and mitochondrial health, the researchers employed a refined self-referencing measurement mode in single HeLa cells. This approach involved the high-frequency reciprocating motion of a UME between the near-field of the cell surface and the bulk solution. Such a method allows for the real-time updating of the bulk solution reference signal, thereby effectively subtracting systematic errors caused by the irreversible decay of probe response in biological media. This study provides a rigorous methodological framework for the future design of single-cell electrochemical metabolic measurement devices.

Fei Li *et al.* [50] investigated oxidative state imbalances and early mechanisms of oxidative damage in primary cortical neurons under heat stress (37–42 °C), as shown in Figure 7c. They developed a specialized SECM platform equipped with precise temperature control and programmable pulse potentials. This system utilized multiple probes sensitive to O_2, H_2O_2, and hydrophilic redox mediators to monitor neuronal physiological indicators. The study revealed distinct dual physiological effects of mild *versus* severe heat stress on neuronal metabolic flux and reactive oxygen species (ROS) generation. Quantitative data indicated that as environmental temperature rose, neuronal oxygen consumption reached a compensatory maximum at 40 °C to maintain ATP synthesis, but subsequently collapsed rapidly under severe heat stress at 41–42 °C. Simultaneously, extracellular H_2O_2 levels and cell membrane permeability increased significantly starting from 39 °C. Further pharmacological studies demonstrated that while potent free radical scavengers could inhibit excessive ROS accumulation, they could not fully reverse mitochondrial respiratory failure or intracellular calcium overload induced by severe heat stress.

What's more, the multi-parametric nature of SECM is particularly effective for evaluating the physiological impact of chemical stimuli on complex tissue structures. Fei Li *et al.* [51] monitored the comprehensive metabolic and electrophysiological responses of *in vitro* cardiac microtissues to various receptor-targeted cardiovascular drugs, as shown in Figure 7b. The researchers constructed a monitoring platform using high-frequency time-division-multiplexed pulse programs. Within a single scanning cycle, the oxidation current of ferrocenecarboxylic acid (FcCOOH) was used to monitor microscopic topographical oscillations caused by cardiac contraction, while specific reduction and oxidation potentials simultaneously monitored oxygen consumption and H_2O_2 secretion. Upon the addition of isoproterenol to the medium, the *in situ* electrochemical maps captured a cascade of reactions: a sharp increase in local oxygen consumption, a significant acceleration of contraction frequency, and a surge in H_2O_2 release due to accelerated oxidative metabolism. Conversely, the introduction of receptor blockers resulted in a synchronized decline in both respiratory activity and contraction frequency. This

experiment suggests the potential application value of the SECM system for non-invasive cardiac toxicology screening and high-throughput drug efficacy assessment. Fei Li *et al.* [52] later used SECM in feedback and programmable-pulse modes to monitor the early dynamics of Erastin-induced ferroptosis in single human hepatocellular carcinoma (HuH7) cells. They found that during the early course of ferroptosis, the cell membrane structure was gradually destroyed and oxidative stress intensified. Specifically, cell membrane permeability increased continuously, cellular oxygen consumption (respiratory activity) was reduced by half, and H_2O_2 released from the cells exhibited periodic bursts regulated by both mitochondrial activity and membrane integrity. This work quantitatively characterized multiple key parameters during early cellular ferroptosis at the single-cell level.

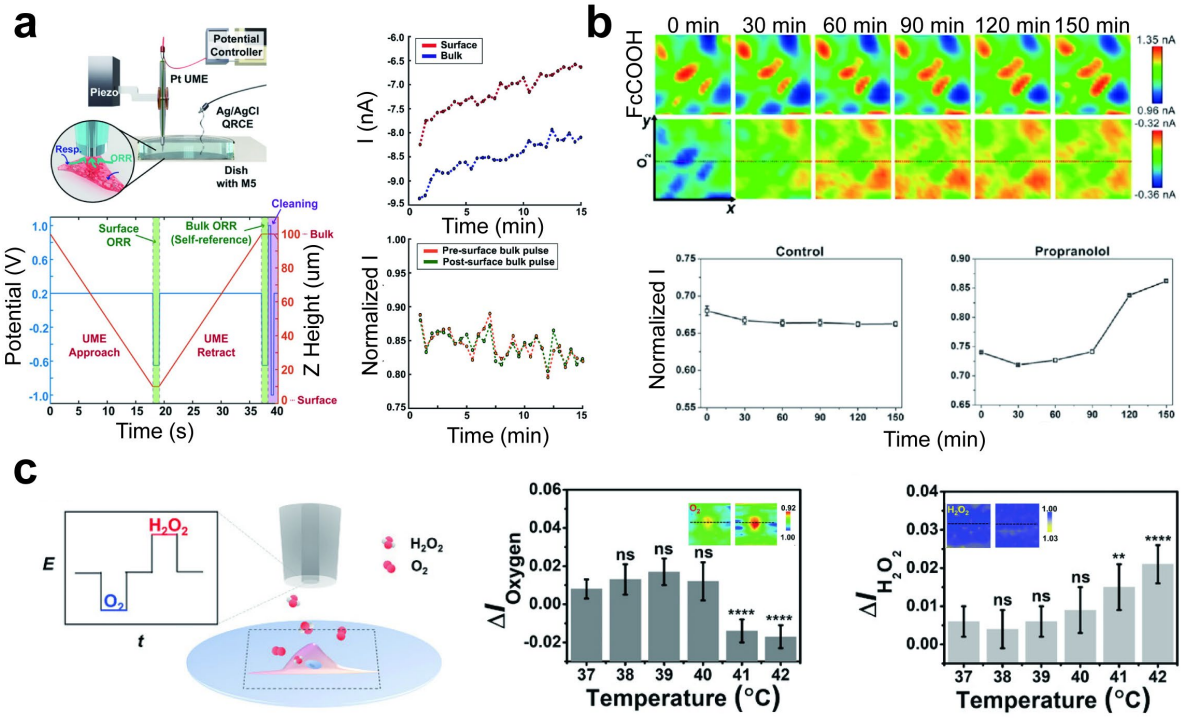

Figure 7. SECM monitoring of cellular metabolism, oxidative stress, and cardiac microtissue responses. **(a)** Illustration of the SECM experimental setup. Temporal profile of a single complete cycle of the self-referencing program. Current recorded for each OCR measurement in the bulk and in the cell vicinity (near-surface), and the near-surface current normalized to the current measured in the bulk, either before the surface pulse or immediately after the surface pulse. Reprinted with permission [49]. Copyright 2023 The Authors; **(b)** SECM images of the topography and oxygen consumption of cardiac tissues without (control) and propranolol (0.5 μM) in the tissue culture from 0 to 150 min using FcCOOH and oxygen as the redox mediators, respectively. Time-course of the normalized probe currents extracted from the SECM images at the red dotted lines. Reprinted with permission [51]. Copyright 2022 American Chemical Society; **(c)** Schematic diagram of SECM with programmable pulse potential mode for characterization of oxygen consumption and extracellular H_2O_2 levels of neurons at different temperatures. Programmable SECM current images and extracted current curves of oxygen reduction and H_2O_2 oxidation of living neurons cultured at 37 °C and after culturing at 37–42 °C for 1 h. Statistical diagrams of the differences in the current responses of oxygen and H_2O_2 across neuron surfaces in the horizontal direction before and after culturing neurons at 37–42 °C for 1 h. Reprinted with permission [50]. Copyright 2022 Wiley-VCH GmbH.

4.3. Interfacial microenvironment analysis of bacterial biofilms

Bacterial biofilms are a typical class of biological soft-matter interfacial systems, composed of bacterial cells, extracellular polymeric substances (EPS), and local chemical gradients. Compared to planktonic bacteria, biofilms exhibit stronger spatial heterogeneity and resilience, with metabolic activity, ion release, oxygen concentration, and antibiotic responses often varying at the micrometer scale. Consequently, relying solely on traditional optical imaging or endpoint staining methods makes it difficult to resolve the dynamic processes at the biofilm interface. SPM can simultaneously provide information on morphology, reaction activity, and mass transport at the microscale, serving as an essential tool for understanding biofilm formation, the mechanisms of antimicrobial materials, and interfacial responses following antibiotic treatment.

Caniglia *et al.* [53] fabricated silver-fluoropolymer (Ag-CFX) antimicrobial films and combined SECM-anodic stripping voltammetry, AFM, and ATR-FTIR to investigate silver ion release and its impact on *Pseudomonas fluorescens* (*P. fluorescens*) biofilm formation. This study reveals that Ag-CFX films release Ag(I) into the aqueous phase, with release kinetics closely tied to the swelling behavior of the polymer matrix; specifically, matrix hydration facilitates the formation of diffusion pathways for silver ions, establishing a localized concentration gradient that interacts with settling bacteria. AFM results demonstrate that surfaces without pre-swelling exhibit lower bacterial coverage, and the morphology of *P. fluorescens* transitions from typical rod-shaped to spherical forms, proving that localized silver ion release exerts significant interfacial stress on the bacteria. Long-term monitoring via ATR-FTIR further indicates that Ag-CFX coatings inhibit biofilm adhesion and growth, although dead cell biomass may serve as a substrate for recolonization in later stages. The core value of this work is reflected in its correlation of local Ag(I) release, material swelling, and biofilm morphological/chemical responses, demonstrating the capacity of coupling SPM with spectroscopic techniques to resolve antimicrobial interfacial mechanisms.

To resolve localized metabolic activity, Darvishi *et al.* [54] employed Soft-Probe-SECM to image the surface electrochemical reactivity of *Escherichia coli* (*E. coli*) biofilms. This method utilizes a flexible microelectrode to scan the biofilm surface in a gentle contact mode, using ferrocene methanol as a redox mediator to construct a metabolic activity map of the biofilm surface layer via feedback mode. This finding proves that *E. coli* biofilms can reduce oxidized ferrocene methanol, thereby generating a higher SECM feedback current than the inert substrate; this signal primarily originates from the surface layer, making the method applicable not only to intact biofilms but also to surface samples obtained through tape stripping. This approach also distinguishes between ampicillin-resistant and non-resistant *E. coli* biofilms and monitors the decline in biofilm activity over time and dosage following gentamicin treatment. This research highlights how Soft-Probe-SECM reduces the perturbation caused by conventional probe scanning in soft biofilms, making microscale electrochemical imaging an effective supplementary means for analyzing the surface metabolic state and antibiotic response of biofilms.

Focusing on the quantification of interfacial mass transport, Klementiev *et al.* [55] developed an SECM-based real-time oxygen gradient measurement method using platinized ultramicroelectrodes to monitor O_2 distribution above *Pseudomonas aeruginosa* (*P. aeruginosa*) biofilms. This study reveals that biofilms can form a hypoxic zone extending hundreds of micrometers above their surface within minutes, with oxygen consumption approaching the maximum mass-transfer rate. Furthermore, even

when treated with high concentrations of ciprofloxacin to kill culturable bacteria, the O_2 gradient and oxygen consumption rate around the *P. aeruginosa* biofilm remain largely unchanged. This result demonstrates that the metabolic microenvironment at the biofilm interface exhibits significant resilience, and the bactericidal effect of antibiotics does not necessarily imply the disappearance of interfacial oxygen-consumption functions. The core value of this study lies in extending SECM from local electrochemical activity imaging to the real-time quantification of external biofilm microenvironment gradients, providing direct evidence for understanding hypoxic niches in chronic infections and antibiotic tolerance.

5. Multidimensional physico-chemical properties measurement at the biological soft matter interface

While SPM enables high-resolution mapping of cellular topology and mechanics under physiological conditions, it lacks the molecular specificity required to correlate physical structures with chemical functions. To address this gap, integrated SPM systems have emerged as a promising approach to achieving non-destructive, multidimensional characterization. These hybrid platforms enable the simultaneous acquisition of morphological and mechanical data, along with specific molecular fingerprints, which is important for interpreting complex biological phenotypes. The value of integrated SPM platforms is not limited to acquiring additional imaging channels; rather, their core value lies in correlating topography, mechanics, chemical composition, and metabolic reactions within the same micro-region, thereby addressing biological questions that are difficult to resolve with a single SPM mode. On the one hand, the combination of AFM with infrared, Raman, or mass spectrometry imaging realizes the precise mapping of chemical fingerprints, such as extracellular polymers, proteins, or lipids, to local adhesion, elastic modulus, and interfacial restructuring processes, as shown in Figure 8; on the other hand, the coupling of SECM with AFM or SICM establishes a correlative coupling between metabolic fluxes, including oxygen consumption, ion release, and redox mediator transformation, and surface topography or microstructural heterogeneity while maintaining precise spatial registration. Compared to standalone SPM techniques that provide only topographic, mechanical, or electrochemical signals, integrated platforms are better suited to precisely characterize structures, detect functions *in situ*, and elucidate their synergistic evolution laws within soft biological interfaces. This fusion of multidimensional information provides a more rigorous perspective for mechanistic analysis of bacterial biofilms, extracellular matrices, and antimicrobial material interfaces.

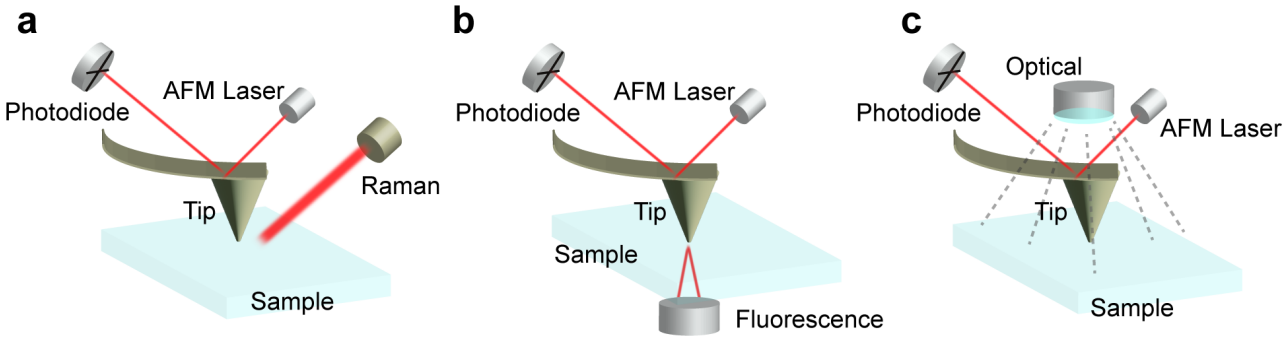

Figure 8. The scheme of integrated SPM platforms. **(a)** The integration of AFM and Raman; **(b)** The integration of AFM and fluorescence; **(c)** The integration of AFM and optical microscopy.

The inherent limitations of SPM in identifying molecular components have motivated the development of integrated techniques such as Tip-Enhanced Raman Spectroscopy (TERS). By combining the chemical sensitivity of Raman scattering with the spatial resolution of SPM, TERS can map molecular compositions on biological surfaces. Mrđenović *et al.* [56] employed AFM-TERS to investigate human pancreatic cancer cell membranes. Their work identified distinct domains enriched with phospholipids, cholesterol, and specific proteins. By analyzing localized Raman intensities, such as histidine (1532 cm^{-1}) and phenylalanine (1001 cm^{-1}) peaks, they provided direct visual evidence of dynamic molecular clusters. This study contributes significantly to the field by validating the "lipid raft" hypothesis through high-resolution observations of coexisting membrane components. Further expanding the technical versatility of these platforms, He *et al.* [57] developed an SICM integrated with TERS, as shown in Figure 9. Using a gold-coated nanopipette and ion-current feedback, they achieved contactless nano-spectroscopic imaging of soft materials such as PDMS. Their research highlights the feasibility of high-resolution chemical mapping without mechanical perturbation, offering a robust framework for investigating delicate biological interfaces.

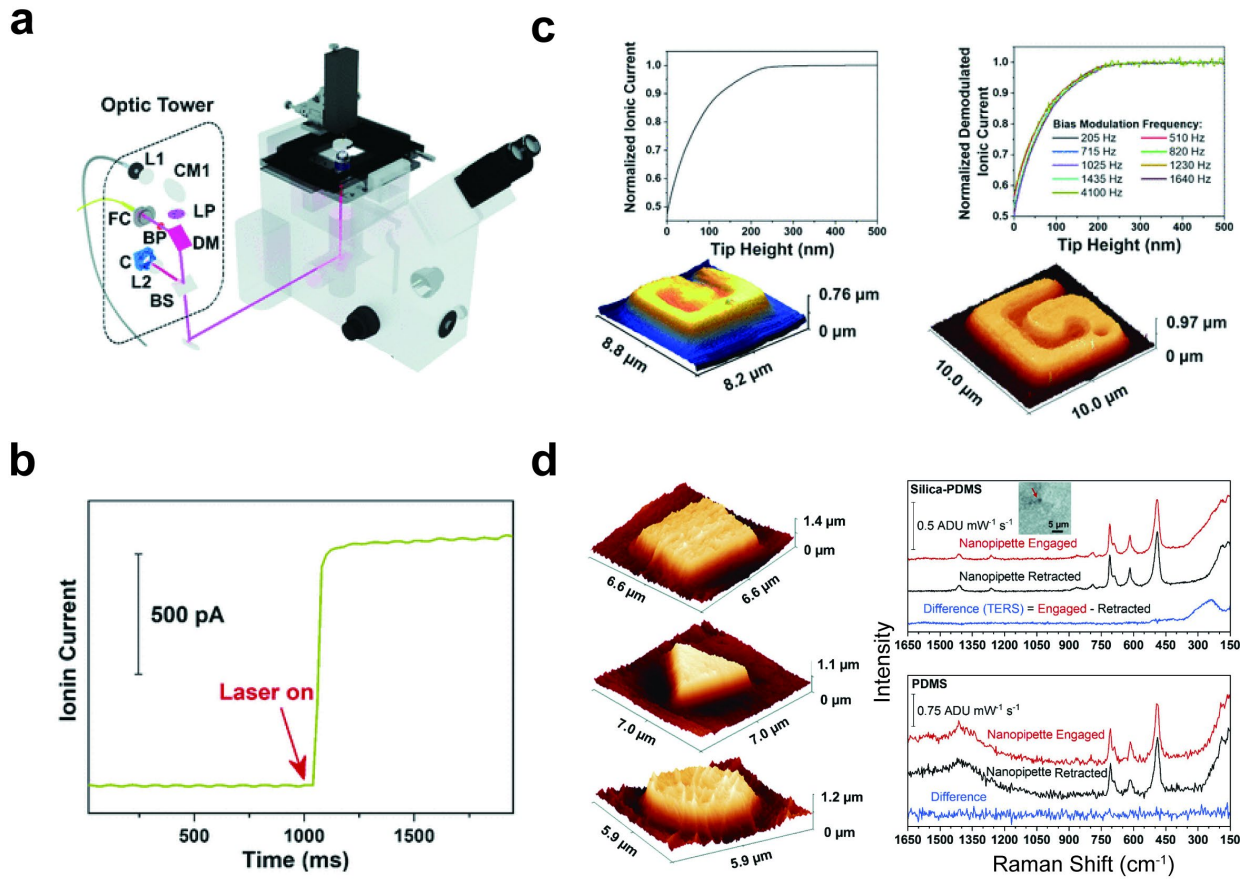

Figure 9. Integrated SICM-TERS platform for contactless nanoscale chemical mapping. **(a)** Overview of SICM-TERS instrument; **(b)** The ionic current response to a 10 mW 785 nm laser focused at the plasmonic nanopipette apex; **(c)** Direct-current (DC) SICM approaching curve and topographic image of a PDMS square spiral protrusion, and bias-modulated alternating-current SICM approaching curve and topographic image; **(d)** Three-dimensional representation of the DC-SICM image of a 5 µm square, triangle, and circle from the PDMS stamp. SICM-TERS of the silica-nanosphere-decorated PDMS with a 785 nm near-IR laser excitation. Reprinted with permission [57]. Copyright 2025 The Authors.

Beyond Raman techniques, the integration of fluorescence microscopy is important for tracking specific protein dynamics. Moura *et al.* [58] demonstrated the power of this correlation by combining differential spinning disk (DSD) fluorescence with AFM to study live-cell co-cultures. Their research focused on the biophysical differences between Saos-2 cells and GFP-tagged MG-63 cells. They found that MG-63 cells exhibited a significantly lower Young's modulus compared to the non-fluorescent Saos-2 cells. These findings correlate mechanical softness with higher proliferative activity and lower differentiation in tumor phenotypes. This study exemplifies how hybrid SPM techniques can help phenotype cells in multi-component systems by linking macroscopic mechanical attributes to microscopic molecular expression.

6. Summary and outlook

SPM has developed into a versatile toolkit for measuring biological soft matter interfaces under conditions that approach their native biological state. AFM provides nanoscale force and mechanical information, SECM maps local electrochemical reactivity and metabolic fluxes, and SICM enables non-contact topographic and ionic measurements on delicate living systems. Together, these techniques bridge the gap between ensemble bioanalytical methods and local interfacial processes. Recent applications show that SPM can quantify viscoelasticity in hydrogels and polymer brushes, resolve receptor-ligand and pathogen-host interactions, visualize membrane proteins and secretory events, and monitor cellular respiration, oxidative stress, and cardiac microtissue responses. These studies suggest that nanoscale physical and electrochemical readouts can provide mechanistic information that is difficult to obtain from conventional optical or bulk electrochemical measurements alone.

Future progress will depend on addressing several key technical bottlenecks, among which establishing a rigorous standardization framework is the most urgent priority to ensure reproducibility across different laboratories. (1) Higher-speed and lower-noise instrumentation is needed to follow transient biological processes without perturbing soft samples. (2) Integrated platforms that combine SPM with spectroscopy, fluorescence imaging, and microfluidics should improve molecular specificity while preserving nanoscale spatial resolution. (3) Standard protocols for probe and cantilever calibration must be unified, particularly for high-speed and ultra-soft cantilevers. (4) Uniform metrics for nanopipette and ultramicroelectrode characterization, such as geometry verification via standard electron microscopy or benchmark cyclic voltammetry, are required to secure stable electrochemical and ionic feedback. (5) The choices of force-curve fitting parameters and contact mechanics models must be constrained; laboratories should implement consistent indentation depths and approach rates to avoid artificial variances when extracting the viscoelastic moduli of soft boundaries. (6) Open-access, automated data-processing pipelines should be developed to handle large-scale mechanical and flux imaging datasets, minimizing the user-dependent bias introduced during manual baseline corrections and peak detection.

Beyond standardization, transitioning SPM from low-throughput, expert-dependent tools to automated, high-throughput bioanalytical platforms represent another critical frontier. Future research should prioritize integrating automated region-of-interest identification with data-driven scanning strategies. By coupling real-time optical/fluorescence imaging with machine learning algorithms, the SPM probe can be dynamically guided to autonomously track mobile cellular targets, navigate complex topography, or identify chemically active hot spots in dense samples while minimizing tip wear and sample damage. Concurrently, the throughput must be scaled up via parallelized probe arrays and microfluidic-integrated

automated sample feeding, enabling statistically robust, population-scale single-cell screening. Furthermore, to fully unlock the power of these multidimensional datasets, improved quantitative and constitutive modeling tailored to live-cell systems must be developed. This requires moving away from overly simplified, static elastic theories toward dynamic, non-linear viscoelastic models that explicitly account for active cytoskeletal remodeling, cytosolic fluid flow, and fluctuating transmembrane molecular transport under true physiological stresses.

In conclusion, biological soft matter interfaces are dynamic entities defined by a seamless coupling of mechanical resilience and electrochemical reactivity. Future research priorities must shift from purely optimizing isolated spatial resolutions to pioneering automated, high-throughput, and data-driven correlative imaging platforms. Accelerating the synergy among scanning probe methods, predictive computational modeling, and complementary technologies such as advanced microfluidics will transform SPM from an interpretive profiling tool into a predictive, quantitative platform. Such a conceptual transformation will ultimately bridge the remaining gaps between local nanoscale interfacial discoveries and macroscale biomedical translations, unlocking new frontiers in cellular mechanobiology, real-time disease diagnosis, and precision therapeutics.

Declaration of generative AI and AI-assisted technologies

During the preparation of this manuscript, the authors used AI-assisted tool only to improve language and readability. Specifically, the authors used Grammarly for language polishing only in limited sections of the manuscript. The intellectual content of the manuscript (including ideas, analysis, and conclusions) is original work, and the manuscript complies with academic integrity and publication ethics standards.

Acknowledgments

This work was financially supported by the National Natural Science Foundation of China (Grant No. 22425403, 22421001).

Authors' contribution

Conceptualization, R.W.; methodology, R.W. and R.L.; validation, R.W. and R.L.; formal analysis, R.W. and R.L.; investigation, R.L.; resources, R.W.; writing—original draft preparation, R.L.; writing—review and editing, R.W.; visualization, R.L.; supervision, R.W.; project administration, R.W.; funding acquisition, R.W. All authors have read and agreed to the published version of the manuscript.

Conflicts of interest

Rui Wen holds the position of Editorial Board Member for *Life Analysis* and has not peer reviewed or made any editorial decisions for this paper. The authors declare no other conflicts of interest.

References

[1] Bowser MT. Introduction to new frontiers in bioanalytical chemistry. *Chem. Rev.* 2013, 113(4):2267–2268.

[2] Mathey F. Analytical and bioanalytical chemistry. *Anal. Bioanal.Chem.* 2002, 372:1.

[3] Koch W. Ten years of analytical and bioanalytical chemistry. *Anal. Bioanal. Chem.* 2012, 402:1.
[4] Chandrasekaran S, Danos N, George UZ, Han JP, Quon G, *et al.* The axes of life: a roadmap for understanding dynamic multiscale systems. *Integr. Comp. Biol.* 2021, 61(6):2011–2019.
[5] Shi P, Azorin-Peris V, Echiadis AS, Zheng J, Zhu Y, *et al.* Non-contact reflection photoplethysmography towards effective human physiological monitoring. *J. Med. Biol. Eng.* 2010, 30(3):161–167.
[6] Dufrêne YF, Ando T, Garcia R, Alsteens D, Martinez-Martin D, *et al.* Imaging modes of atomic force microscopy for application in molecular and cell biology. *Nat. Nanotechnol.* 2017, 12(4):295–307.
[7] Matuszewski BK, Constanzer ML, Chavez-Eng CM. Strategies for the assessment of matrix effect in quantitative bioanalytical methods based on HPLC-MS/MS. *Anal. Chem.* 2003, 75(13):3019–3030.
[8] Icha J, Weber M, Waters JC, Norden C. Phototoxicity in live fluorescence microscopy, and how to avoid it. *Bioessays* 2017, 39(8):1700003.
[9] Garcia R, Proksch R. Nanomechanical mapping of soft matter by bimodal force microscopy. *Eur. Polym. J.* 2013, 49(8):1897–1906.
[10] Tseng AA, Notargiacomo A, Chen TP. Nanofabrication by scanning probe microscope lithography: a review. *J. Vac. Sci. Technol. B* 2005, 23(3):877–894.
[11] McConney ME, Singamaneni S, Tsukruk VV. Probing soft matter with the atomic force microscopies: imaging and force spectroscopy. *Polym. Rev.* 2010, 50:235–286.
[12] Xie Q, Xu XG. What do different modes of AFM-IR mean for measuring soft matter surfaces? *Langmuir* 2023, 39(49):17593–17599.
[13] Jandt KD. Atomic force microscopy of biomaterials surfaces and interfaces. *Surf. Sci.* 2001, 491(3):303–332.
[14] Alsteens D, Gaub HE, Newton R, Pfreundschuh M, Gerber C, *et al.* Atomic force microscopy-based characterization and design of biointerfaces. *Nat. Rev. Mater.* 2017, 2(5):17008.
[15] Chen X, Li B, Liao Z, Li, J, Li X, *et al.* Principles and applications of liquid-environment atomic force microscopy. *Adv. Mater. Interfaces* 2022, 9(35):2201864.
[16] Shi X, Qing W, Marhaba T, Zhang W. Atomic force microscopy—scanning electrochemical microscopy (AFM-SECM) for nanoscale topographical and electrochemical characterization: principles, applications and perspectives. *Electrochim. Acta* 2020, 332:135472.
[17] Minopoli A, Evangelista D, Marras M, Perini G, Palmieri V, *et al.* Viscoelastic interpretation of AFM nanoindentation for predicting nanoscale stiffness in soft biomaterials. *Polym. Test.* 2025, 153:109026.
[18] Wang H, Zhang H, Da B, Lu D, Tamura R, *et al.* Mechanomics biomarker for cancer cells unidentifiable through morphology and elastic modulus. *Nano Lett.* 2021, 21(3):1538–1545.
[19] Makarova N, Sokolov I. Cell mechanics can be robustly derived from AFM indentation data using the brush model: error analysis. *Nanoscale* 2022, 14(11):4334–4347.
[20] Kontomaris SV, Malamou A. Hertz model or Oliver & Pharr analysis? Tutorial regarding AFM nanoindentation experiments on biological samples. *Mater. Res. Express* 2020, 7(3):033001.
[21] Heath GR, Micklethwaite E, Storer TM. NanoLocz: image analysis platform for AFM, high-speed AFM, and localization AFM. *Small Methods* 2024, 8(10):2301766.
[22] Schitter G, Åström KJ, DeMartini BE, Thurner PJ, Turner KL, *et al.* Design and modeling of a high-speed AFM-scanner. *IEEE Trans. Control Syst. Technol.* 2007, 15(5):906–915.

[23] Ando T. Techniques developed for high-speed AFM. In *Control Technologies for Emerging Micro and Nanoscale Systems*, 1st ed. Berlin: Springer, 2011. pp. 1–16.
[24] Chan FY, Kurosaki R, Ganser C, Takeda T, Uchihashi T. Tip-scan high-speed atomic force microscopy with a uniaxial substrate stretching device for studying dynamics of biomolecules under mechanical stress. *Rev. Sci. Instrum.* 2022, 93(11):12.
[25] Ando T. High-speed AFM imaging. *Curr. Opin. Struct. Biol.* 2014, 28:63–68.
[26] Zoski CG. Review-advances in scanning electrochemical microscopy (SECM). *J. Electrochem. Soc.* 2016, 163(4):H3088–H3100.
[27] Barker AL, Unwin PR. Measurement of solute partitioning across liquid/liquid interfaces using scanning electrochemical microscopy-double potential step chronoamperometry (SECM-DPSC): principles, theory, and application to ferrocenium ion transfer across the 1,2-dichloroethane/aqueous interface. *J. Phys. Chem. B* 2001, 105(48):12019–12031.
[28] Liu R, Shen Z, Wen R, Wan L. Recent advances in the application of scanning probe microscopy in interfacial electroanalytical chemistry. *J. Electroanal. Chem.* 2023, 938:117443.
[29] Morkvenaite-Vilkonciene I, Ramanaviciene A, Ramanavicius A. Redox competition and generation-collection modes based scanning electrochemical microscopy for the evaluation of immobilised glucose oxidase-catalysed reactions. *RSC Adv.* 2014, 4(91):50064–50069.
[30] Anariba F, Anh JH, Jung GE, Cho NJ, Cho SJ. Biophysical applications of scanning ion conductance microscopy (SICM). *Mod. Phys. Lett. B* 2012, 26(5):1130003.
[31] Gorelik J, Ali NN, Sheikh Abdul Kadir SH, Lab M, Stojkovic P, *et al.* Non-invasive imaging of stem cells by scanning ion conductance microscopy: future perspective. *Tissue Eng. Part C Methods* 2008, 14(4):311–318.
[32] Nastenko AA, Kolmogorov VS, Vaneev AN, Gorelkin PV, Klyachko NL, *et al.* Scanning ion conductance microscopy for living cell nanomechanics: principles, advances and applications. *Anal. Methods* 2026, 18(8):1583–1593.
[33] Ma L, Wei Y, Wang N, Chen W, Lu Y. Soft matter photonics: interplay of soft matter and light. *ACS Nano* 2025, 19(12):11501–11516.
[34] Baulin VA, Giacometti A, Fedosov DA, Ebbens S, Varela-Rosales NR, *et al.* Intelligent soft matter: towards embodied intelligence. *Soft Matter* 2025, 21(21):4129–4145.
[35] Neri-Cruz CE, Teixeira FME, Gautrot JE. A guide to functionalisation and bioconjugation strategies to surface-initiated polymer brushes. *Chem. Commun.* 2023, 59(49):7534–7558.
[36] Eroglu A, Laçin O, Yildirim E. Fabrication of PAA-co-PNIPAm brushes via surface-initiated-PET-RAFT polymerization and investigation of their dual responsive behavior. *RSC Adv.* 2025, 15(46):38876–38888.
[37] Dokukin ME, Kuroki H, Minko S, Sokolov I. AFM study of polymer brush grafted to deformable surfaces: quantitative properties of the brush and substrate mechanics. *Macromolecules* 2017, 50(1):275–282.
[38] Ge L, Jin G, Fang X. Investigation of the interaction between a bivalent aptamer and thrombin by AFM. *Langmuir* 2012, 28(1):707–713.
[39] Liu J, Zhang X, Yang H, Yuan J, Wei H, *et al.* Study of the interactions between endolysin and bacterial peptidoglycan on *S. aureus* by dynamic force spectroscopy. *Nanoscale* 2015, 7(37):15245–15250.

[40] Koehler M, Aravamudhan P, Guzman-Cardozo C, Dumitru AC, Yang J, *et al.* Glycan-mediated enhancement of reovirus receptor binding. *Nat. Commun.* 2019, 10(1):4460.
[41] Formosa-Dague C, Fu Z, Feuillie C, Derclaye S, Foster TJ, *et al.* Forces between Staphylococcus aureus and human skin. *Nanoscale Horiz.* 2016, 1(4):298–303.
[42] Knoops B, Becker S, Poncin MA, Glibert J, Derclaye S, *et al.* Specific interactions measured by AFM on living cells between peroxiredoxin-5 and TLR4: relevance for mechanisms of innate immunity. *Cell Chem. Biol.* 2018, 25(5):550–559.
[43] Schröder U, Harnisch F. Life electric—nature as a blueprint for the development of microbial electrochemical technologies. *Joule* 2017, 1(2):244–252.
[44] Liang T, Gu C, Fang J, Xu D, Wang Z, *et al.* Cellular metabolism biosensing: from extracellular microenvironment to intracellular physiology monitoring. *Biosens. Bioelectron.* 2026, 295:118250.
[45] Lei L, Guo C, Yang H, Hu F. Recent advances in single-cell electrochemical sensing technology: a review. *Microchem J.* 2026, 220:116440.
[46] Jin R, Zhou W, Xu Y, Jiang D, Fang D. Electrochemical visualization of membrane proteins in single cells at a nanoscale using scanning electrochemical cell microscopy. *Anal. Chem.* 2023, 95(27):10172–10177.
[47] Nashimoto Y, Takahashi Y, Ida H, Matsumae Y, Ino K, *et al.* Nanoscale imaging of an unlabeled secretory protein in living cells using scanning ion conductance microscopy. *Anal. Chem.* 2015, 87(5):2542–2545.
[48] Song Y, Zhang S, Cao C, Yan J, Li M, *et al.* Imaging structural and electrical changes of aging cells using scanning ion conductance microscopy. *Small Methods* 2024, 8(8):2301315.
[49] Cremin K, Meloni GN, Valavanis D, Soyer OS, Unwin PR. Can single cell respiration be measured by scanning electrochemical microscopy (SECM)? *ACS Meas. Sci. Au* 2023, 3(5):361–370.
[50] Zhang J, Liu Y, Li Y, Zhu T, Qiu J, *et al. In situ* and quantitatively imaging of heat-induced oxidative state and oxidative damage of living neurons using scanning electrochemical microscopy. *Small Methods* 2022, 6(12):2200689.
[51] Li Y, Ye Z, Zhang J, Zhao Y, Zhu T, *et al.* In situ and quantitative monitoring of cardiac tissues using programmable scanning electrochemical microscopy. *Anal. Chem.* 2022, 94(29):10515–10523.
[52] Zhao Y, Li Y, Kuermanbayi S, Liu Y, Zhang J, *et al. In situ* and quantitatively monitoring the dynamic process of ferroptosis in single cancer cells by scanning electrochemical microscopy. *Anal. Chem.* 2023, 95(3):1940–1948.
[53] Caniglia G, Sportelli MC, Heinzmann A, Picca RA, Valentini A, *et al.* Silver-fluoropolymer (Ag-CFX) films: Kinetic study of silver release, and spectroscopic-microscopic insight into the inhibition of *P. fluorescens* biofilm formation. *Anal. Chim. Acta* 2022, 1212:339892.
[54] Darvishi S, Pick H, Oveisi E, Girault HH, Lesch A. Soft-probe-scanning electrochemical microscopy reveals electrochemical surface reactivity of *E. coli* biofilms. *Sens. Actuators, B* 2021, 334:129669.
[55] Klementiev AD, Jin Z, Whiteley M. Micron scale spatial measurement of the O_2 gradient surrounding a bacterial biofilm in real time. *mBio* 2020, 11(5):10–1128.
[56] Mrđenović D, Ge W, Kumar N, Zenobi R. Nanoscale chemical imaging of human cell membranes using tip-enhanced Raman spectroscopy. *Angew. Chem., Int. Ed.* 2022, 134(43):e202210288.
[57] He X, Scarabelli L, Chiang N. Construction of a scanning ion-conductance microscope for tip-enhanced Raman spectroscopy. *Anal. Chem.* 2025, 97(30):16098–16103.

[58] Moura CC, Miranda A, Oreffo RO, De Beule PA. Correlative fluorescence and atomic force microscopy to advance the bio-physical characterisation of co-culture of living cells. *Biochem. Biophys. Res. Commun.* 2020, 529(2):392–397.